NUMERIČNA ŠTUDIJA KOEFICIENTA DINAMIČNEGA AKTIVNEGA ZEMELJSKEGA TLAKA ZA KOHEZIVNE ZEMLJINE

Mehrab Jesmani
P.E., Koury Engineering & Testing Inc.
Chino, CA, ZDA
E-pošta: mehrabjesmani@gmail.com

Hossein Alirezanejad
Professional Geotechnical Engineer
Tehran, Iran
E-pošta: h.alirezanejad@gmail.com

Hamed Faghihi Kashani
HyGround Engineering LLC
Williamsburg, MA, ZDA
E-pošta: hamed@hyground.com

Mehrad Kamalzare *(vodilni avtor)*
California State Polytechnic University,
Department of Civil Engineering
3801 West Temple Ave. Pomona, CA 91768, ZDA
E-pošta: mkamalzare@cpp.edu

Ključne besede

koeficient dinamičnega aktivnega zemeljskega tlaka (K_{ae}), kohezivna zaledna zemljina, metoda končnih diferenc (FDM), natezne razpoke, podporni zid, seizmična obtežba

Izvleček

Podporni zidovi so predlagani v mnogih projektih, kot so mostovi, priobalne konstrukcije, cestne konstrukcije in v primerih, ko je potrebno bočno podpiranje izkopov vertikalnih površin. Koeficient aktivnega zemeljskega tlaka K_a, predstavlja pomemben parameter pri študiju statičnega in dinamičnega obnašanja podpornih zidov. Mnoge študije obravnavajo ta koeficient v statičnih pogojih, v mnogih predhodnih dinamičnih študijah so raziskovalci obravnavali obnašanje nekohezivne zaledne zemljine ali pa so naredili poenostavljene predpostavke za kohezivne zaledne zemljine (npr.: psevdo statični pogoji). V tej študiji je bila preučevana vrednost koeficienta aktivnega zemeljskega tlaka (K_a) v polni dinamični situaciji (K_{ae}). Podporni zid s kohezivno zaledno zemljino je preučevan z uporabo metode končnih diferenc (FDM), upoštevani so vplivi pomembnih lastnosti zemljine in obtežb. Model je zasnovan z Mohr-Coulomb modelom kriterija porušitve pri seizmični obtežbi. Rezultati kažejo, da je vrednost koeficienta K_{ae} na vrhu zidu, kjer je zelo občutljiv na kakršno koli spremembo lastnosti zemljine in obtežbe, večja od vrednosti koeficienta K_{ae} zaradi visoke vrednosti tlaka povzročenega s horizontalnim dinamičnim pospeškom in prisotnostjo nateznih razpok.

NUMERICAL STUDY OF THE DYNAMIC ACTIVE LATERAL EARTH PRESSURE COEFFICIENT OF COHESIVE SOILS

Mehrab Jesmani
P.E., Koury Engineering & Testing Inc.
Chino, CA, USA
E-mail: mehrabjesmani@gmail.com

Hossein Alirezanejad
Professional Geotechnical Engineer
Tehran, Iran
E-mail: h.alirezanejad@gmail.com

Hamed Faghihi Kashani
HyGround Engineering LLC
Williamsburg, MA, USA
E-mail: hamed@hyground.com

Mehrad Kamalzare *(corresponding author)*
California State Polytechnic University,
Department of Civil Engineering
3801 West Temple Ave. Pomona, CA 91768, USA
E-mail: mkamalzare@cpp.edu

Keywords

Dynamic active lateral earth pressure coefficient (K_{ae}), cohesive backfill soil, finite difference method (FDM), tension cracks, retaining wall, seismic loading

Abstract

Retaining walls are proposed in many projects, such as bridges, coastal structures, road constructions and wherever lateral support is required for the vertical surface of an excavation. The active lateral pressure coefficient of soil, K_a, is an important parameter for studying the static and dynamic behaviors of these retaining walls. Many studies have evaluated this coefficient in static situations, but in most previous dynamic studies, researchers have worked on the behavior of cohesionless backfill soil or made simplifying assumptions (e.g., pseudo-static status) for cohesive soils as backfill soil. In this study, the size of the active lateral earth pressure coefficient (K_a) was studied in a full dynamic situation (K_{ae}). A retaining wall with cohesive backfill soil is evaluated using the finite-difference method (FDM) and the effects of important soil and loading properties are assessed. The model is based on Mohr-Coulomb failure criteria under seismic loading. The results show that the value of K_{ae} at the top of the wall, where it is highly sensitive to any variation in the soil and loading properties, is greater than one due to the high pressure value induced by the horizontal dynamic acceleration and the presence of tension cracks.

List of Symbols

K_a	The active lateral earth pressure coefficient of soil
K_{ae}	Dynamic Active Lateral Earth Pressure Coefficient
K_h	Horizontal seismic pseudo-static coefficient
K_v	Vertical acceleration coefficients of the seismic loading
B	Width of the wall foot
H	Height of the wall
G	Shear Modulus
c	Cohesion
i	Backfill Soil Angle

1 INTRODUCTION

The active lateral earth pressure coefficient of soil (Ka) has been the subject of intense interest and study for the design of retaining walls. Coulomb [1], as the first scientist to study the backfill soil pressure, assumed that the effective pressure that builds up behind a retaining wall is the result of the weight of a soil section above a certain linear sliding plane and used the limit equilibrium theory of forces (Fig. 1) to assign the active and passive pressures. The general equations developed through this theory are based on a number of fundamental assumptions as follows: the retained soil is cohesionless (no clay component), homogeneous (not a varying mixture of materials), isotropic (similar stress-strain properties

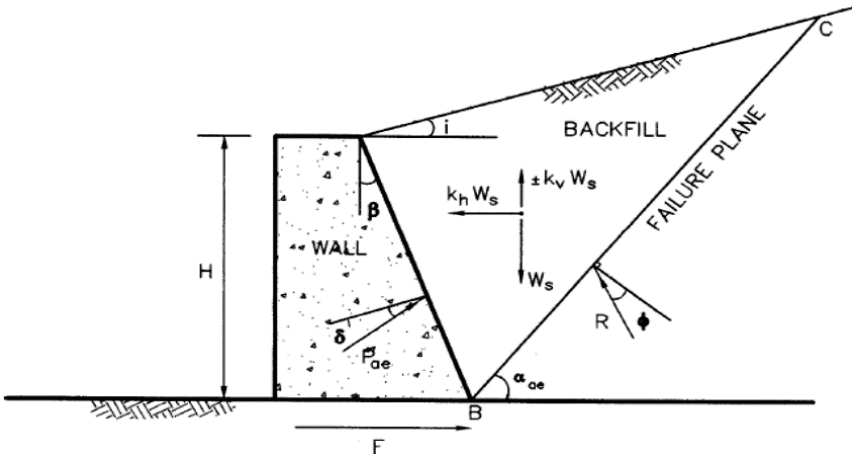

Figure 1. Limit equilibrium theory of retaining walls (Coulomb 1776, [1]).

in all directions or in practical terms, not reinforced), semi-infinite (the wall is very long and the soil moves back a long distance without bends or other boundary conditions), and well drained (to avoid a consideration of pore pressure). Accordingly, he suggested Eq. 1 for the static loading condition:

$$K_a = \frac{\cos^2(\varphi-\theta)}{\cos^2\theta\cos^2(\delta+\theta)\left[1+\sqrt{\frac{\sin(\delta+\varphi)\sin(\varphi-\beta)}{\cos(\delta+\theta)\cos(\theta-\beta)}}\right]^2} \quad (1)$$

where δ is the friction angle between the soil and the wall, φ is the internal friction angle and β and θ are as defined in Fig.1.

Rankine [2] suggested a stress-field solution to predict the active and passive earth pressures. His methodology relied on the assumptions that the soil is cohesionless, the wall is frictionless, the soil-wall interface is vertical, the failure surface on which the soil moves is planar and the resultant force is angled parallel to the backfill surface. He proposed Eq. 2 for determining K_a in the case when the backfill soil has a zero angle with respect to the horizon and Eq. 3 for the cases where the backfill soil has a non-zero angle to the horizon, both equations considering the static loading only:

$$K_a = \frac{1-\sin\varphi}{1+\sin\varphi} = \tan^2\left(\frac{\pi}{2}-\frac{\varphi}{2}\right) \quad (2)$$

$$K_a = \cos i\frac{\cos i-\sqrt{\cos^2 i-\cos^2\varphi}}{\cos i+\sqrt{\cos^2 i-\cos^2\varphi}} \quad (3)$$

where φ is the internal friction angle and i is the backfill soil angle with respect to the horizon.

Okabe [3] and Mononobe and Matuso [4] conducted pseudo-static analyses and suggested a relationship between K_a and some other parameters, as indicated in Eq. 4, known as the M-O equation. This equation, which can be considered as a development of Eq. 1 (Coulomb 1776), has been mainly used for the study of dry and non-cohesive soils under earthquake loading conditions.

$$K_{ae} = \frac{\cos^2(\varphi-\theta-\beta)}{\cos\theta\times\cos^2\beta\times\cos(\beta+\delta+\theta)\times D} \quad (4)$$

where φ is the internal friction angle, β is the internal steep of the wall, δ is the friction angle between the wall and the backfill soil and D and θ are as defined in Eq. 5 and Eq. 6 , respectively.

$$D = \left[1+\sqrt{\frac{\sin(\varphi+\delta)\sin(\varphi-\theta-i)}{\cos(\delta+\beta+\theta)\cos(i-\beta)}}\right]^2 \quad (5)$$

$$\theta = \tan^{-1}\left[\frac{k_h}{1-k_v}\right] \quad (6)$$

where i is the angle between the backfill soil and the horizontal (the slope of the soil face) and K_h and K_v are the horizontal and vertical acceleration coefficients of the seismic loading, respectively.

Saran and Prakash [5] developed the M-O equation (Eq. 4) for cohesive backfill soils, neglecting the earthquake vertical acceleration. Their model showed, however, the independence of the maximum pressure from the backfill soil weight over the failure plane, making the solution insecure from a practical viewpoint. Later, Zarrabi-Kashani [6] suggested an equation for assigning the angle of failure wedge in seismic loading conditions,

based on the M-O equation. Wood [7] examined the behavior of a solid retaining wall (without collapsing) under the active seismic pressure of the backfill soil using an elasto-plastic method. He stated that the resultant of the dynamic pressure is located at a point 0.6 times the wall height from the wall toe and the sliding plane has a curved shape. Steedman and Zeng [8] carried out a pseudo-static analysis to evaluate the behavior of retaining walls higher than 10 meters. In an attempt to address the deficiency of the pseudo-static analysis for evaluating the displacement of retaining walls under a seismic loading, Richards and Elms [9, 10] suggested a method to investigate the main ground motivating parameters caused by seismic loading (with maximum speed) to decrease the active seismic soil pressure based on the wall displacement.

Richards and Shi [11] presented an analytical solution for determining the lateral active pressure in cohesive soils, which was in fact a development of the elasto-plastic equation for cohesionless soils. They studied the effects of both horizontal and vertical accelerations. Velesos and Younan [12] reported that in solid walls that have elastic limitations in their foundation the magnitude and distribution of the backfill soil pressure are related to the limited flexibility of the foundation. Morisson and Ebeling [13] simulated the dynamic passive earth pressure by using a limited equilibrium computation with a logarithmic spiral failure surface. Soubra [14] assessed the passive earth pressure coefficients of rigid retaining structures in static and seismic loading conditions using an upper bound limit analysis. Chen [15] studied the problem of earthquake-induced lateral earth pressure using the LRFD method. Kumar [16] tried to determine the seismic passive earth pressure coefficient for sands. Kumar and Chitikela [17] employed the method of characteristics to evaluate the passive earth pressure coefficient in seismic loading conditions. Green and Ebeling [18] used the finite-difference method (FDM) (FLAC software) to evaluate the dynamic pressure on a retaining wall in dry consolidated sandy soils. They also drew an analogy between the lateral earth pressure coefficients (K_{ae}) obtained from FLAC software and the M-O equation, as shown in Fig. 2.

Saran and Gupta [19] continued the method of Saran and Prakash [5] in retaining walls having backfill soil with a slope in order to determine the lateral active pressure for cohesive soils. Cheng [20] studied the seismic lateral earth pressure coefficients for c-φ soils by employing the slip-line method. Yang and Yin [21] studied the seismic passive earth pressure by applying the limited analysis method with a non-linear failure criterion. Choudhury and Nimbalkar [22] investigated the temporal effects and shear phase changes of the primary waves behind the retaining walls by using a pseudo-dynamic method. Mylonakis et al. [23] proposed an alternative for the M-O equation for an evaluation of the seismic earth pressure on gravity walls with cohesionless backfill soil. Ghanbari and Ahmadabadi [24] brought forth two equations for perusing the inclined retaining walls backfilled by cohesionless and cohesive soils with a friction angle, via both static and pseudo-static methods. They declared that the active earth pressure in soils with friction and cohesion has a nonlinear distribution in the seismic loading condition.

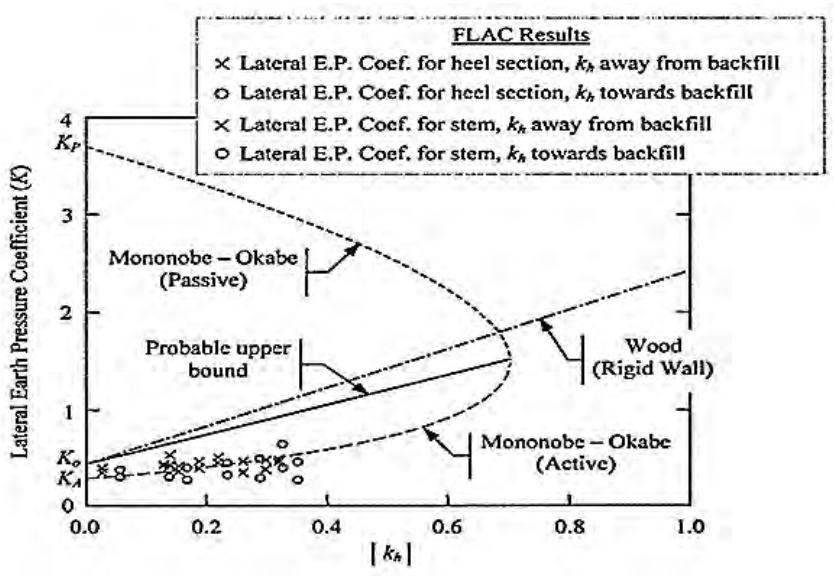

Figure 2. Comparison between lateral earth pressure coefficient (K_a) obtained from FLAC Software and M-O Equation [18].

Most of the above-mentioned works, with similarities in the standpoint through which the issue was looked at, namely, either assessing the cohesionless soils or using a pseudo-static method, shared basic assumptions on which ground their models were resting: a) negligible friction between the wall and the cohesive soil, b) single surface failure plane, c) adequate wall movement under the minimum active lateral pressure, d) using Mohr-Coulomb shear strength: $s = c + \sigma \tan\varphi$ (where s stands for the shear impedance, c for the cohesion, φ for the friction angle and σ for the effective stress of the backfill soil), e) backfill soil behaving like a solid material and f) the negligible effect of the tension cracks.

In this work, by considering the shortages felt in the context and with the aim of approaching a more realistic model, we studied the retaining walls with cohesive backfill soil under a full dynamic loading by means of a numerical model. What are the effects of the tension cracks, which in theory are supposed to increase the static active lateral pressure in the range 20 to 40% [25,26]. The results presented herein could be of great interest and avail in different sectors of geotechnical engineering, such as road construction, building construction and coastal structures in locations with cohesive soils.

2 DEFINITION OF NUMERICAL MODEL AND ASSUMPTIONS

The model retaining wall (B/H= 0.15, B: Width of the wall foot, H: Height of the wall) is made of concrete (Table 1) with the geometrical properties defined in Table 2. The wall is resting on a non-collapsing basic layer (elastic layer) and is facing a vertical surface of cohesive soil (Table 3) that is considered as a semi-infinite, homogenous and uniform environment. Since the length of the wall is a multiple of its height, the wall is modeled two dimensionally with the plane-strain condition and is subjected to a seismic loading on its unit length with constant acceleration and different ratios of k_v / k_h , i.e., 0, $1/3$ and $2/3$. To simulate the real condition that a wall would experience during an earthquake, the seismic load was applied as an acceleration, and at the same moment, to all of the nodes at the bottom of the model. Furthermore, for modeling the stress-strain behavior of the soil, the elasto-plastic model of the Mohr-Coulomb failure criteria was exploited.

Table 1. Concrete properties.

Bulk Modulus (K) $10^6 \times$ kPa	Poisson's Ratio (v)	Shear Modulus (G) $10^6 \times$ kPa	Unit weight (γ) kPa
13.9	0.2	10.4	25

Table 2. Geometrical properties of retaining walls and related parameters.

Height (H) m	Ratio of width to height (B/H)	Normalized depth by wall height (Z/H)	Backfill soil angle from horizontal (i°)
3,5,8	0.15	0–1	0,10,20,30,60

Table 3. Backfill soil properties of studied retaining walls (Poisson's ratios (v) for all soils are equal to 0.4).

Cohesion (c) kPa	Elasticity Modulus (E) kPa	Dry unit weight (γ_d) kN/m^3	Friction angle (φ°)
25	5000	16.5	5.15
45	12000	17.5	5.15
85	20000	18.5	5.15
100	27000	19.5	5.15

3 FINITE-DIFFERENCE MODEL STRATEGIES

A two-dimensional computational model is used under the plane-strain condition. Interface elements were used to model the shear stiffness, friction, cohesion, etc. for soil interfacing surfaces. Fig. 3 illustrates the interfacing elements for interfacing surfaces (soil to soil and soil to wall) of this study.

The interface elements are used to model the shear stiffness, friction, cohesion between two different surfaces. These elements are necessary to model and for simulating any probable separation, or the sliding of surfaces. However, the behavior of the soil-to-soil, or soil-to-concrete interfaces is a function of the internal friction angle, and therefore, the properties of the interface elements were defined in such a way as to account for this. The elements and their properties were applied to the model from the beginning and before analyzing the model.

Fig. 4 shows the interface element used in this research. In the figure, T is the tension strength, k_n is the vertical stiffness, k_s is the shear stiffness, and S is the shear strength.

In accordance with the node velocity, which is related to the amount of damping force, in order to avoid the problems of wrong element appropriation for damping (such as generated body forces in failure areas that could create some errors) and to avoid the allocation of a constant damping to every element, the nodal unbalanced force damping system was used in the model with a D (damping factor) value of 5%. Since dynamic analyses with unreal boundaries can cause a reflection of the waves in the computing area, individual dashpots have been used for the boundary nodes to absorb the body waves without any reflection.

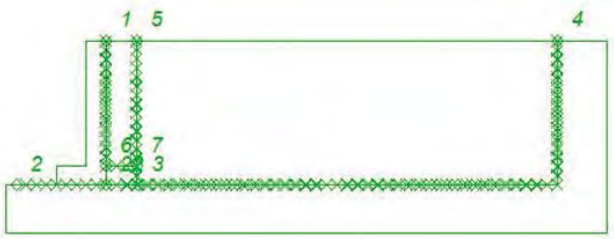

Figure 3. Interface elements of the wall-soil system in the model.

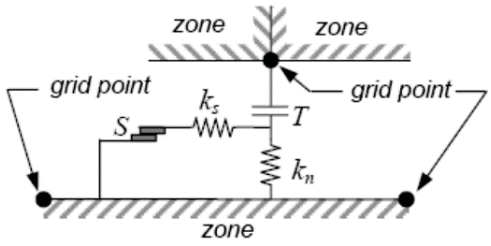

Figure 4. Interface element used in this study.

3.1 Meshing and loading condition

The meshes of the model for all the parts were squares with a dimension of 0.2 meter. In the static loading condition, the model was equilibrated with the materials weight. The lower nodes of the basic soil were restrained in the vertical and horizontal directions and it was assumed that the soil displacements do not affect the places beneath the defined nodes. Moreover, the nodes of the vertical boundaries were only restrained in the horizontal direction (Fig. 5).

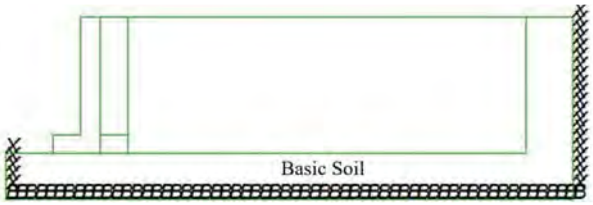

Figure 5. Model boundary condition in static loading.

In the dynamic loading condition, when the model is considered to be statically balanced, the dynamic load affects all the nodes of the base soil simultaneously (Fig. 6). In this situation, the displacement of the meshing nodes is taken to be equal to zero, in order to determine the net dynamic displacement after the loading. In addition, the wall was permitted to move, to develop an active condition and subsequently, the maximum value of K_{ae} experienced by the wall was recorded by the software as the dynamic active lateral pressure. The free

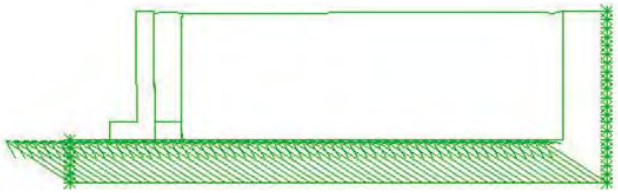

Figure 6. Load effect on all nodes of base soil layer with constant acceleration in dynamic loading.

Figure 7. Free field boundaries condition in dynamic loading.

fields of the model are taken as Fig. 7, which introduces the elements such that their masses are concentrated in nodes, and absorb the waves as free field boundaries.

4 MODEL VERIFICATION

In order to confirm the validity of the results achieved during the current study, a dry sandy soil with properties defined in Table 4 was modeled with the FDM (finite-difference method) analysis using FLAC. The results were compared with what the M-O equation predicts (as a proven equation confirmed and used by many experimental and numerical analyses). Interestingly, good agreement was found to exist between the two, from which results, a brief demonstration is presented in Fig. 8 (with K_h = 0.1~0.3, K_v = 0.1, c = 0 kPa and H = 3m). It is seen that with an increase in the internal friction angle, K_{ae} decreases. On the other hand, K_{ae} (dynamic active lateral earth pressure coefficient) increases when K_h increases (comparison of Fig. 8a, 8b and 8c). From the agreement found with the M-O equation and also from the logical trend of K_{ae} changes with the corresponding parameters, evaluated by this model, the validity of the FDM analysis can be ruled out.

Table 4. Granular soil properties used for the model verification.

ν	γ-- (kN/m^3)	c (kPa)	$\varphi°$	Tension resistance (T)	$\psi°$
0.3	15, 16.5, 18, 19.5, 20	0	25, 30, 35, 40, 45	0	0

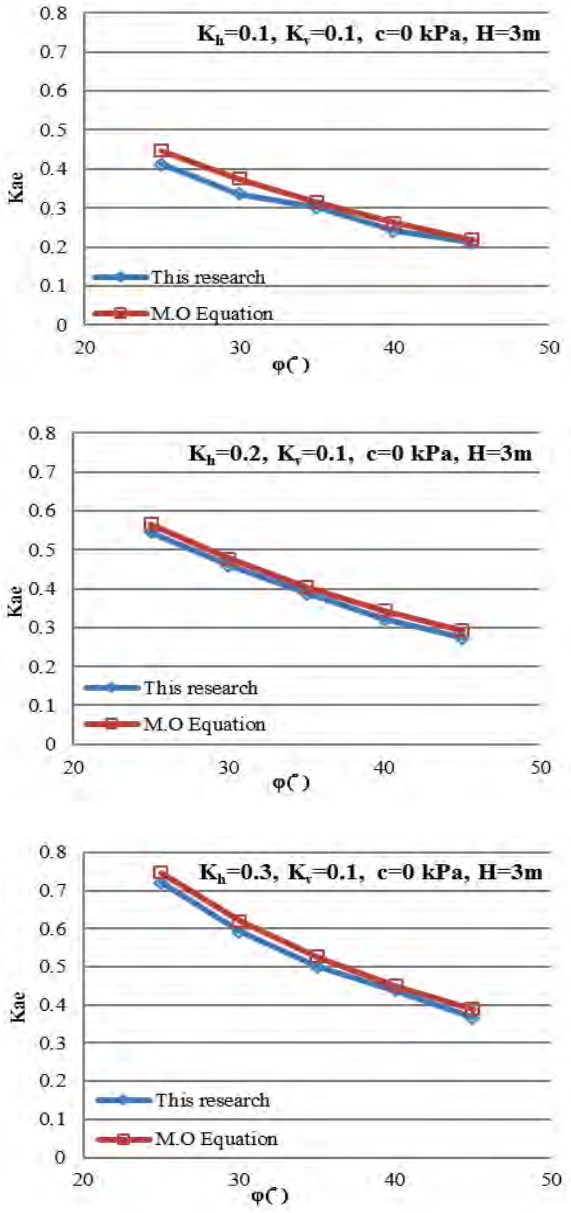

Figure 8. K_{ae} variation vs. φ for results obtained by numerical model of this research and M-O equation for constant K_v and different K_h coefficient.

5 RESULTS AND DISCUSSION

In this section, firstly, the effects of different parameters on K_{ae} are discussed in the two-dimensional condition and then, the parameters recognized as highly influential on K_{ae} are discussed in three-dimensional graphs with more details. Finally, some important "two-variable functions" will be proposed for the evaluation of the effective parameters.

5.1 Two-dimensional evaluation

5.1.1 Evaluation of dynamic active lateral earth pressure coefficient on the retaining wall

As seen in Fig. 9, in the dynamic loading condition the soil displacement at the top of the wall is more than that at the bottom and this difference is caused by the inconstant value of K_{ae} along the height. The lateral earth pressure at the top of the wall is affected by the backfill clayey soil tension cracks and at the bottom it is affected by the soil sliding caused by the upper soil layers' weight. At the top of the wall, K_{ae} is greater than 1 and it decreases gradually toward the depth.

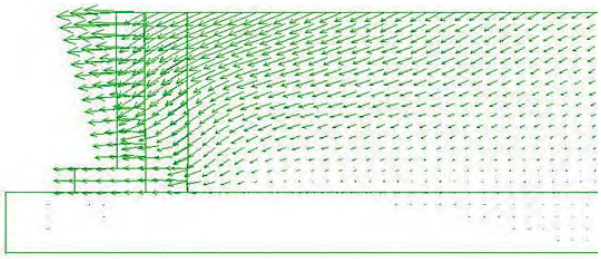

Figure 9. Displacement of the wall during seismic loading (φ = 15°, c = 45 kPa, K_v = 0.2 and, K_h = 0.3).

5.1.2 Effect of the soil depth on K_{ae}

The variation of K_{ae} with normalized depth by height (Z/H) for different cohesions and K_v/K_h ratios is shown in Fig. 10. It is apparent that K_{ae} decreases as the depth increases. This reduction appears sharply on the top of the wall and then slows down at the middle. At the bottom of the wall, K_{ae} starts increasing again; probably due to the soil sliding caused by the weight of the upper soil layers. Moreover, it is observed throughout Fig. 10 that for normalized depth (Z/H) values higher than approximately 0.16, Kae becomes less than 1 ($K_{ae} \leq 1$), for Z/H in the range of 0.25 to 0.75, K_{ae} remains almost constant and for Z/H larger than 0.75, K_{ae} starts increasing.

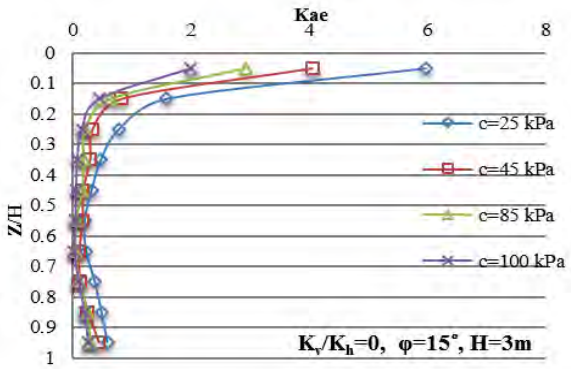

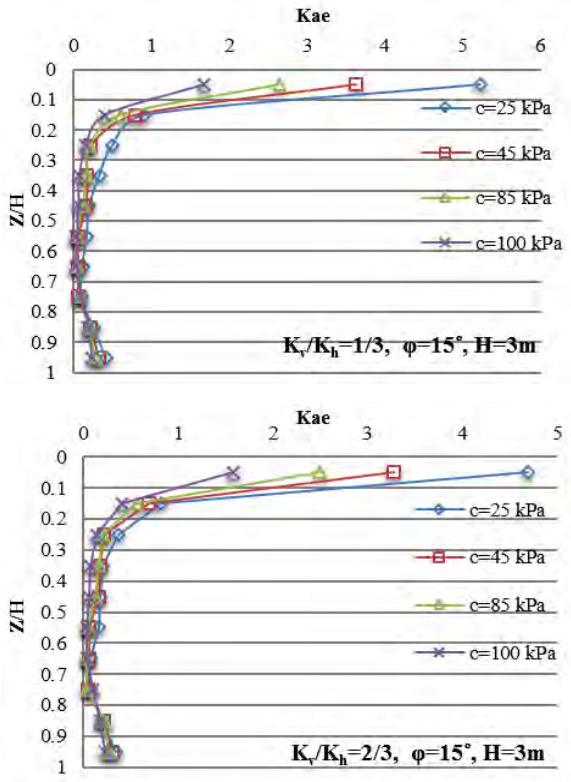

Figure 10. The variation of dynamic active lateral pressure coefficient (K_{ae}) vs. normalized depth Z/H for different cohesions and K_v/K_h ratios.

5.1.3 Effect of the soil cohesion on K_{ae}

As presented in Fig. 11, having a K_v/K_h ratio, a wall height (H), an internal friction angle ($\varphi°$) and a normalized depth (Z/H) constant, an increase in cohesion (c), will decrease K_{ae}. A reduction of the soil sliding and displacement as a result of the cohesion increase between the soil particles could be the reason for such behavior. In addition, it can be inferred from Figs. 10 and 11 that this effect decreases as the depth increases. Fig. 11 shows that at the top of the wall (Z/H = 0.05), increasing the soil cohesion (c) from 25 to 100 kPa, results in a decrease of about 45% in K_{ae}. Whereas, moving toward the middle of the wall (Z/H = 0.15, 0.35 & 0.65), the reduction rate decreases, indicating that the reduction of the cohesion is highly affected by the depth growth. Considering all the subsets of Figs. 10 and 11 demonstrates that for all cohesion values, Kae is larger than 1 in the first depth zone ($0 < Z/H < 0.1$) and that by increasing the cohesion, the dynamic active lateral pressure coefficient reaches 1 for lower Z/H ratios (lower depths). Therefore, it can be concluded that an increase in the soil cohesion decreases the depth of the tension cracks.

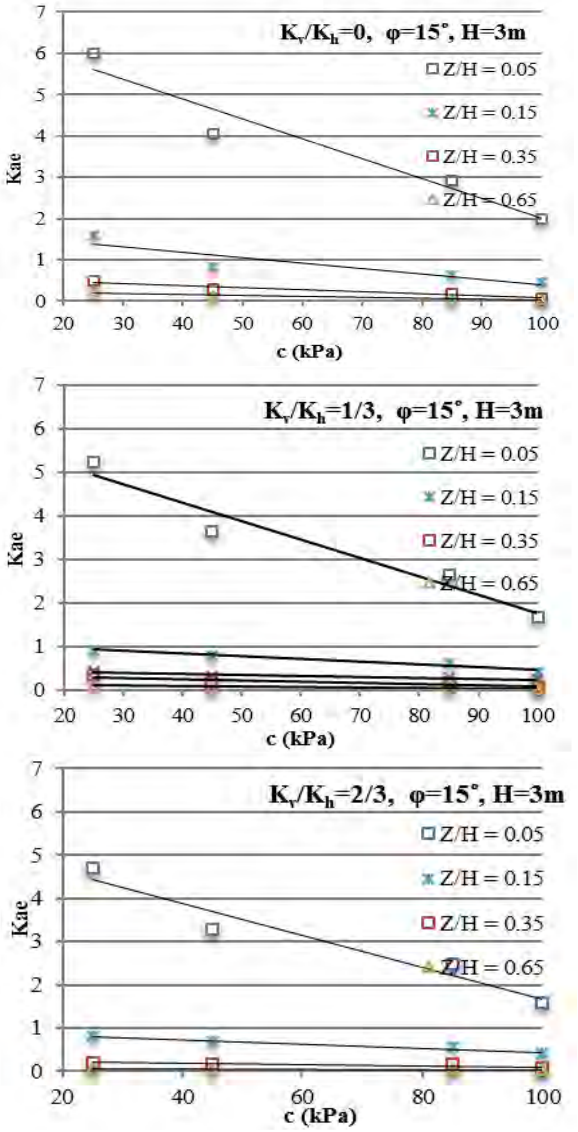

Figure 11. Variation of dynamic active lateral pressure coefficient (K_{ae}) vs. soil cohesion for different normalized depth Z/H and K_v/K_h ratios.

5.1.4 Effect of the K_v/K_h ratio on K_{ae}

As can be seen in Fig. 12, at constant cohesion (c), internal friction angle ($\varphi°$), height (H) and Z/H, a decrease in K_v/K_h ratio results in an increase of the dynamic active lateral pressure coefficient. Although this increase is not significant, it can be inferred that if the vertical acceleration of an earthquake decreases compared to its horizontal acceleration, the destructive effects of the seismic loading would increase. Besides, by increasing the soil cohesion or depth, the effect of the K_v/K_h ratio on K_{ae} becomes less significant (the slope decreases).

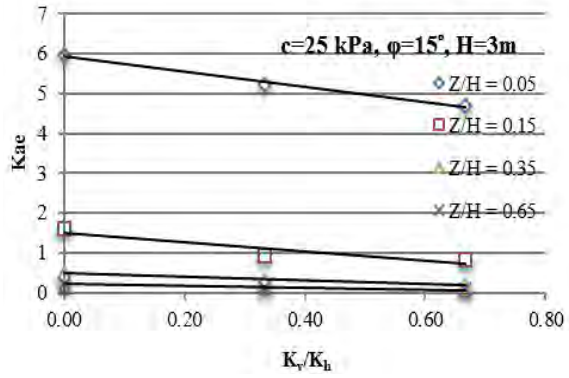

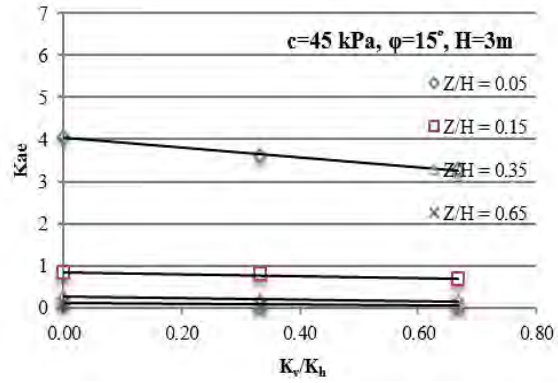

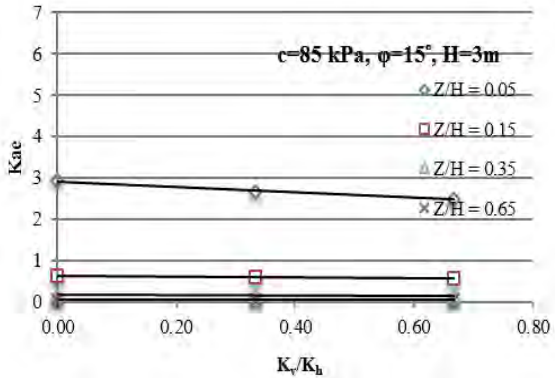

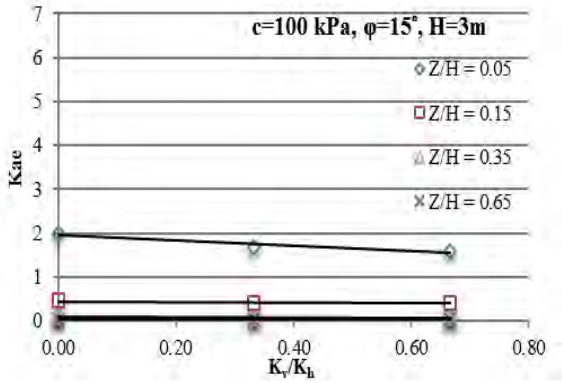

Figure 12. The variation of dynamic active lateral pressure coefficient (K_{ae}) vs. K_v/K_h ratios for different normalized depths Z/H and soil cohesions.

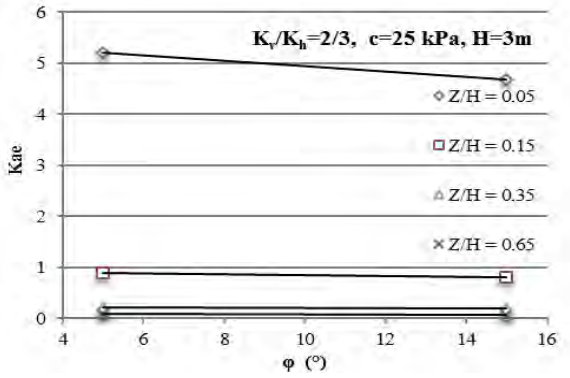

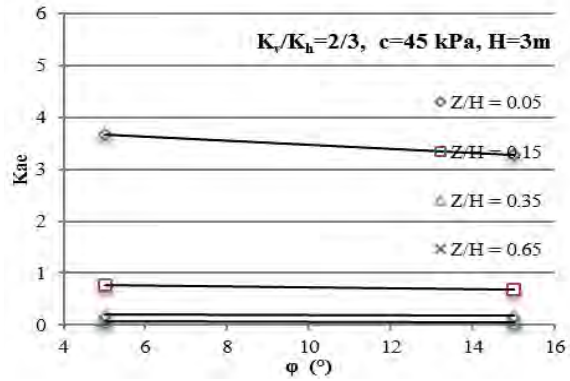

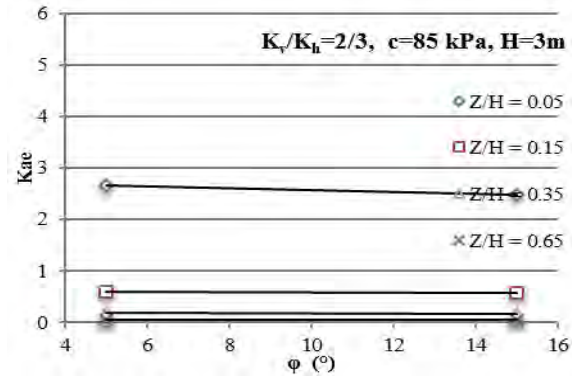

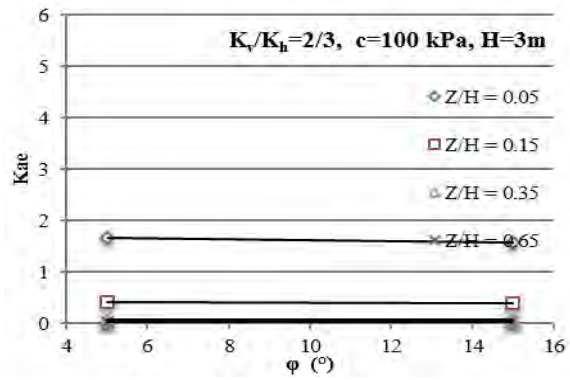

Figure 13. Variation of the dynamic active lateral pressure coefficient (K_{ae}) vs. soil friction angle $\phi°$ for different normalized depths Z/H and soil cohesions.

5.1.5 Effect of the internal friction angle (φ) on K_{ae}

Fig. 13 shows the variation of K_{ae} versus the friction angles (φ°) for different normalized depths (Z/H) and cohesions. It can be inferred that at a constant height (H), cohesion (c), K_v/K_h ratio and Z/H, a diminution in the value of the internal fiction angle from to results in an increases of about 10 to 15% in K_{ae} for lower cohesions (c = 25 and 45 kPa) and about 5 to 7% for higher cohesions (c = 85 and 100 kPa). Since the decreases of the φ can be simply translated to a looser and more collapsible nature of the soil, the likelihood of failing and sliding will obviously increase. Therefore, the dynamic active lateral pressure coefficient increases with a decrease of the friction angle and this effect becomes less significant with the soil cohesion growth and the depth increase.

5.1.6 Effect of the retaining wall height (H) on K_{ae}

Fig. 14 shows the effect of the wall height on K_{ae} in different normalized depths (Z/H) and soil cohesions. As can be seen, K_{ae} increases with the wall height, at constant internal friction angle (φ), cohesion (c), K_v/K_h and Z/H ratios. By increasing the wall height, the effect of the horizontal acceleration of the seismic loading increases at the top of the wall due to the longer moment arm. Moreover, increasing the wall height leads to an increased weight of the backfill soil. Therefore, the displacement at the bottom of the wall increases as a result of the higher elements weight of the backfill soil in comparison with a shorter wall. Fig. 14 also shows that increasing the wall height by 60–67% can induce an increase of about 10 to 38% for K_{ae} at the top of the wall (Z/H = 0.05). In addition, by moving toward the middle of the wall (Z/H = 0.15, 0.35 & 0.65) this incremental rate of K_{ae} decreases as a result of the wall's height increase. It is also obvious that by increasing the soil cohesion, the effect of H on K_{ae} decreases.

5.1.7 Effect of the horizontal acceleration of seismic loading (K_h) on K_{ae}

In order to investigate the effect of K_h on K_{ae}, two values for K_h (0.35 and 0.7) were chosen. As can be seen in Fig. 15 at a constant wall height (H), friction angle (φ), cohesion (c) and K_v, increasing K_h causes an increase of K_{ae} such that a direct relation highlights the destructive effects of the horizontal acceleration of the earthquake compared to its vertical acceleration. Obviously, increasing the horizontal force increases the sliding area of the backfill soil and this in turn leads to a higher value of the dynamic active lateral pressure. Fig. 15 also reveals that increasing the soil cohesion decreases the significance of the influence of K_h on K_{ae}. At the top of the wall (Z/H = 0.05, 0.15), a cohesion growth of 25 or 100 kPa can decrease the increase rate of K_{ae} versus K_h by 5 and 10%, respectively.

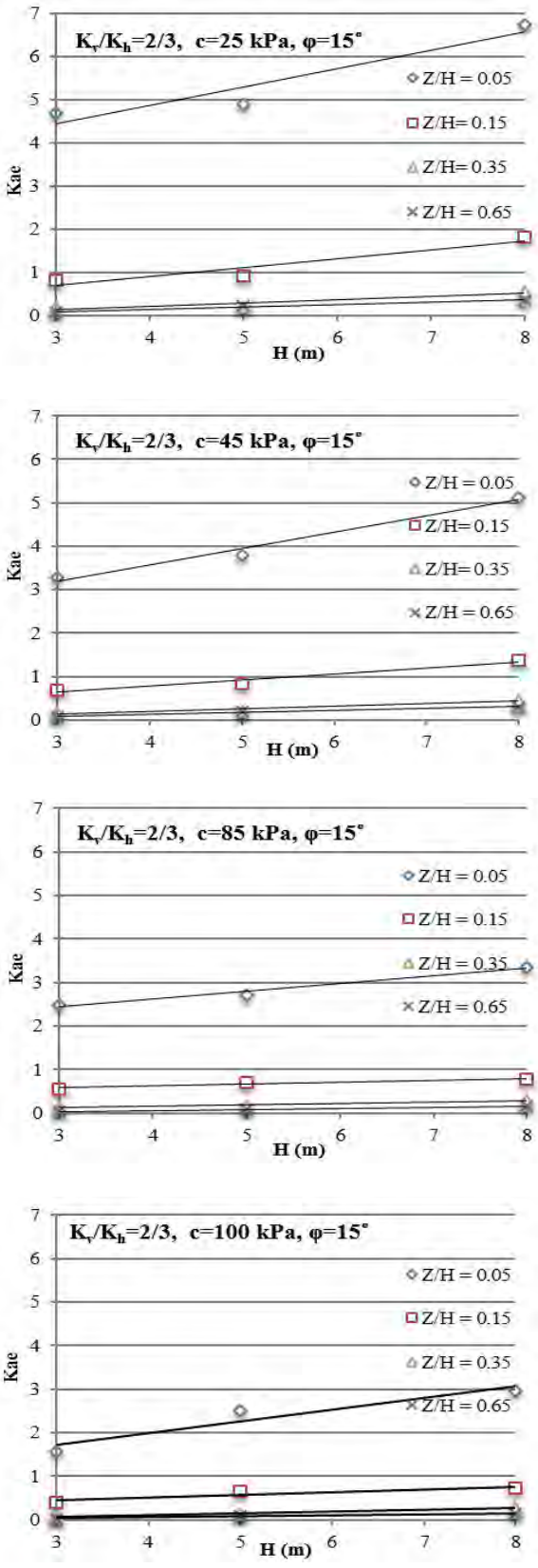

Figure 14. Variation of the dynamic active lateral pressure coefficient (K_{ae}) vs. wall heights (H) for different normalized depths Z/H and soil cohesions.

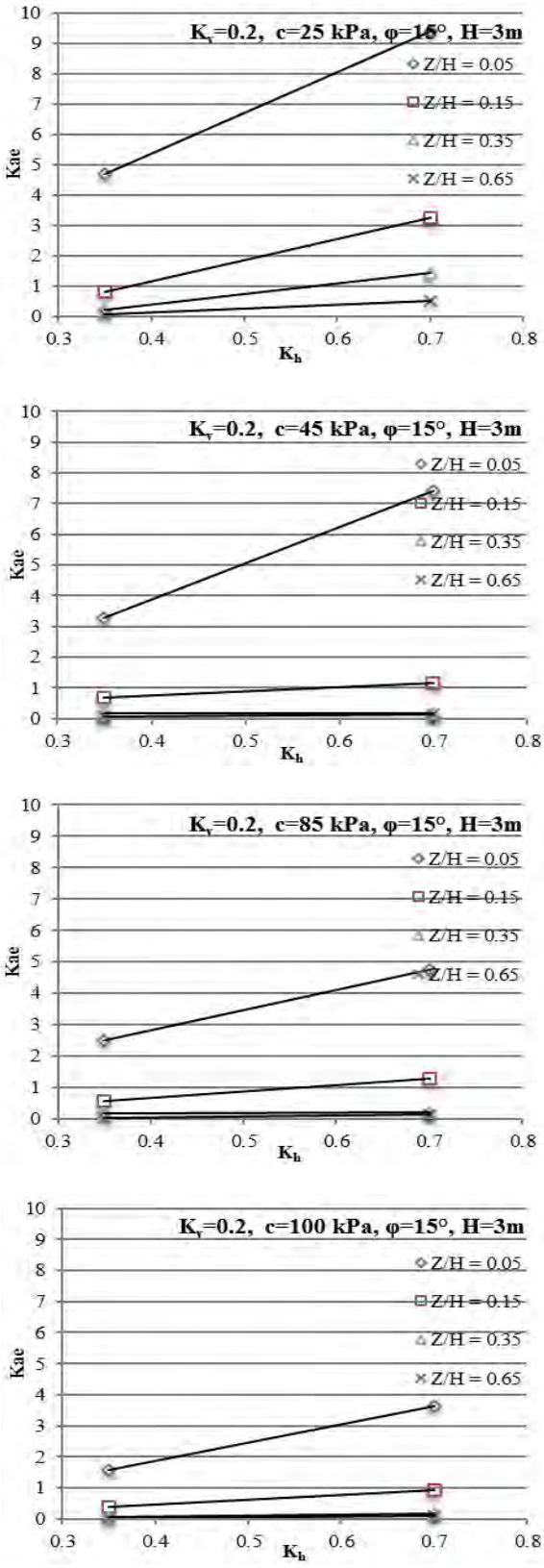

Figure 15. Variation of the dynamic active lateral pressure coefficient (K_{ae}) vs. horizontal acceleration coefficient (K_h) for different normalized depths Z/H and soil cohesions.

5.1.8 Effect of the backfill soil angle (i) on K_{ae}

Fig. 16 suggests that at constant K_v/K_h ratio, cohesion (c), friction angle (φ), height (H) and Z/H, an increase of the backfill soil angle with the horizon (i), makes K_{ae} increase almost linearly. It is clear that the horizontal

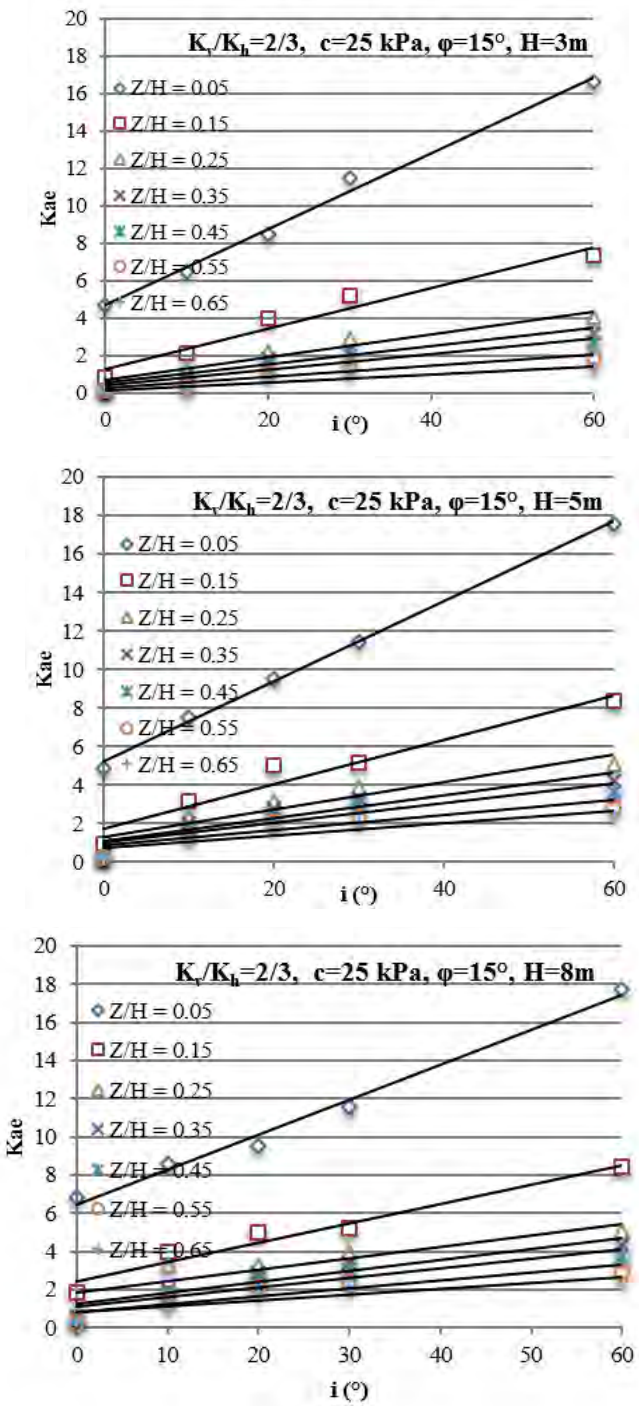

Figure 16. Variation of the dynamic active lateral pressure coefficient (K_{ae}) vs. backfill soil angles measured from horizontal (i) for different normalized depths Z/H ratios and wall heights (H).

acceleration component of the earthquake increases with the slope of the backfill soil and hence, increases K_{ae}. Fig. 16 also confirms that the effect of i on K_{ae} diminishes with the depth growth and the height of the wall does not have a significant effect on the variation of K_{ae} versus i. Moreover, in the upper section of the walls, for Z/H = 0.05 and 0.15, the variation of K_{ae} versus i is significant and the slope of this increment is approximately equal to 0.2 and 0.11 for all the walls, respectively. Accordingly, in the upper section of the wall, increasing the backfill soil angle from 0 to 60 degrees can increase K_{ae} linearly with the mentioned slope. Furthermore, going toward the depth, the effect of i on K_{ae} becomes negligible.

5.2 Three-dimensional graphs and two variable functions

In this section the effect of some critical parameters on K_{ae} is discussed, with the backfill soil surface being considered parallel to the ground surface (i = 0°), except in the section where i is a variable.

5.2.1 Effect of the K_v/K_h ratio and normalized depth (Z/H) on K_{ae}

Fig. 17 shows the effects of K_v/K_h and the normalized depth (Z/H) on K_{ae}, simultaneously. As can be seen clearly, for high depth ratios (K_v/K_h) the variation of K_v/K_h does not have a significant effect on K_{ae}. Whereas, for depth ratios less than about 0.15, K_{ae} becomes highly sensitive to K_v/K_h ratio variations with a potential increase possibility of up to a value of 6.

Eq. 7 is proposed to give an approximation for K_{ae} by certain values of K_v/K_h ratio and normalized depth (Z/H) (for depth ratios less than 0.75 and soil cohesion of 25 to 45 kPa);

$$K_{ae} = \frac{800}{\left[1+\left(\frac{\frac{k_v}{k_h}+3}{2.55}\right)^2\right]\left[1+\left(\frac{\frac{Z}{H}+0.04}{0.011}\right)^2\right]} \quad (7)$$

5.2.2 Effect of the ratio and soil cohesion on Kae

Fig. 18 is a combination of Fig. 11 and 12. As mentioned in the two-dimensional section, by increasing the K_v/K_h ratio and the soil cohesion, K_{ae} decreases. Fig. 18 clearly shows how the increase of the soil cohesion decreases the effect of the K_v/K_h ratio on K_{ae} variations. It is also apparent that for a low soil cohesion, K_{ae} is highly sensitive to a K_v/K_h ratio variation.

Considering the noticeable effect of the K_v/K_h ratio and the cohesion on K_{ae} in a two-dimensional study at the top of the wall, Eq. 8 is proposed to give an approximation for the active lateral earth pressure coefficient using certain values of the K_v/K_h ratio and the normalized soil cohesion (by 100 kPa) for depth ratios equal to and less than 0.05;

$$K_{ae} = \frac{680}{\left[1+\left(\frac{\frac{c(kPa)}{100}+3}{0.20}\right)^2\right]\left[1+\left(\frac{\frac{k_v}{k_h}+4}{2.6}\right)^2\right]} \quad (8)$$

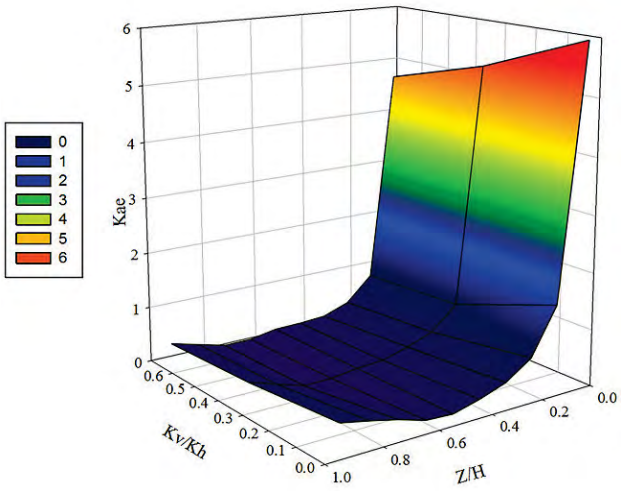

Figure 17. Variation of the dynamic active lateral pressure coefficient (K_{ae}) vs. K_v/K_h ratios and normalized depth Z/H in 3D perspective (i = 0°, φ = 15°, c = 25kPa).

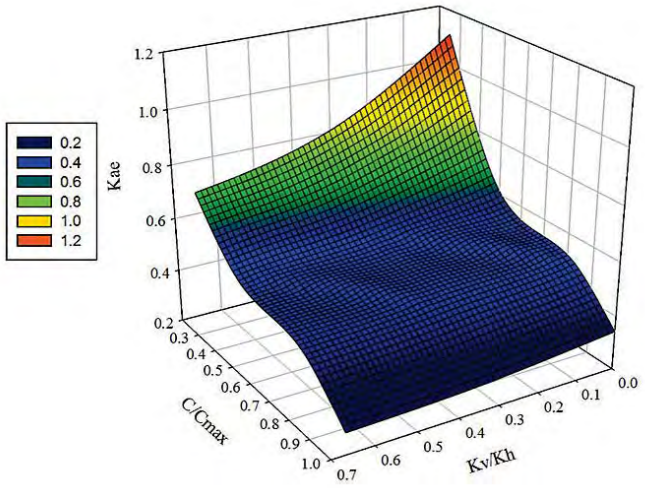

Figure 18. Variation of the dynamic active lateral pressure coefficient (K_{ae}) vs. K_v/K_h ratios and normalized soil cohesion c/c_{max} in 3D perspective (i = 0°, φ = 15°).

5.2.3 Effect of the normalized depth (*Z/H*) and the soil cohesion on K_{ae}

Fig. 19 shows the effect of the normalized soil cohesion and the depth ratio on K_{ae} It indicates that at high depth ratios the effect of the soil cohesion variation on K_{ae} is negligible. As discussed earlier in the two-dimensional section, the effect of soil cohesion on K_{ae} is significant at depth ratios of less than 0.15 (at the top the wall), with the possibility to increase K_{ae} up to a high value such as 5. This can be attributed to an increase of the tension cracks' depth due to the soil cohesion depression.

The 3D graph derived from the variations of K_{ae} versus the depth ratio and the normalized soil cohesion (by c_{max} = 100 kPa) shows a good fit to Eq. 9 for depth ratios (*Z/H*) less than 0.75 and K_v/K_h ratios between *1/3* and *2/3*;

$$K_{ae} = \frac{1675}{\left[\left[1+\left(\frac{\frac{Z}{H}+0.03}{0.015}\right)^2\right]\left[1+\left(\frac{\frac{c(kPa)}{100}+0.91}{0.36}\right)^2\right]\right]} \quad (9)$$

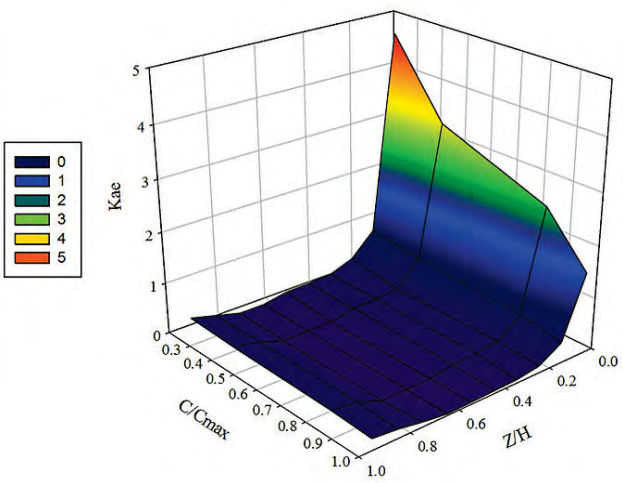

Figure 18. Variation of the dynamic active lateral pressure coefficient (K_{ae}) vs. normalized depth *Z*/*H* and normalized soil cohesion c/c_{max} in 3D perspective (i = 0°, φ = 15°).

6 CONCLUSION

The behavior of the retaining wall with cohesive backfill soil was evaluated using the finite-difference method (FDM), and the effects of different soil and loading properties on Kae were investigated. The following specific conclusions can be drawn:

1. The magnitude of K_{ae} for cohesive soils is larger than 1 at the top of the wall and becomes less than 1 at the middle and bottom of the wall.
2. Increasing the soil cohesion (c) in the range 25 to 100 kPa reduces K_{ae} by approximately 45% at the top of the wall (Z/H = 0.05) and by moving toward the bottom of the wall this reduction rate decreases.
3. By decreasing the K_v/K_h ratio, in the same zones of the wall height the effect of c on K_{ae} becomes more severe.
4. By decreasing the K_v/K_h ratio, the dynamic active lateral pressure coefficient increases insignificantly. Moreover, increasing the soil cohesion or depth makes this effect even more negligible.
5. With a reduction of the internal fiction angle from 15° to 5°, K_{ae} increases about by 10–15% at lower cohesions (c = 25 and 45 kPa) and around 5–7% at higher cohesions (c = 85 and 100 kPa).
6. Increasing the wall height by 60–70% can increase K_{ae} by about 10–38% at the top of the wall and by moving toward the middle of the wall this rate decreases.
7. By increasing the vertical acceleration relative to the horizontal acceleration in seismic loading (K_v/K_h ratio), the depth of tension cracks in backfill soil decreases.
8. By increasing the soil cohesion, the effect of K_h on variations of K_{ae} decreases. At the top of the wall (Z/H = 0.05, 0.15), a cohesion growth between 25 and 100 kPa can decrease the increscent rate of K_{ae} versus K_h between 5 and 10 percent.
9. By increasing the backfill soil angle with horizon (i), K_{ae} increases. The effect of i on K_{ae} decreases with the depth growth and the height of the wall does not have a significant effect on the variation of K_{ae} versus i.
10. K_{ae} is extremely sensitive to the variation of the soil and loading properties at the top of the wall (Z/H < 0.15).

Acknowledgement

The authors would like to show their gratitude to Koury Engineering & Testing, Inc. The authors also would like to thank Mr. Armin Jesmani for his hard work and help to provide the graphs, mathematical equations, and organizing the structure of this paper.

REFERENCES

[1] Coulomb, C.A. 1776. Essai sur une application des regles de maximia et minimis a quelques problemes de statique relatifs a l'architecture. Mem. Acad. Roy. Div. Sav. 7, 343-387.

[2] Rankine, W.M. J. 1857. On the Stability of Loose Earth. Philos Trans R Soc London, Part 1, pp. 9-27.
[3] Okabe, S. 1924. General theory of earth pressure and seismic stability of retaining wall and dam. Japan Soc. Civil Eng. 12, 1, 1277-1323.
[4] Mononobe, N., Matuso, H. 1929. On the determination of earth pressures during earthquakes. Proc. of the World Eng. Conf., Tokyo, Japan, 9, paper No. 388.
[5] Saran, S., Prakash, S. 1968. Dimensionless parameters for static and dynamic earth pressures behind retaining walls. Indian Geotech. J. 7, 3, 295 – 310.
[6] Zarrabi, K. 1973. Sliding of Gravity Retaining Wall During Earthquakes Considering Vertical Acceleration and Changing Inclination of Failure Surface. M.S. Thesis, Department of Civil Engineering MIT, Cambridge, MA.
[7] Wood, J. H. 1973. Earthquake-induced soil pressures on structures. Rep. EARL 73-05, Earthquake Engineering Research Laboratory, California Inst. Of Technol., Pasadena, California, pp. 175-186. DOI: 10.1061/(ASCE)GT.1943-5606.0000351
[8] Steedman, R.S., Zeng, X. 1990. The influence of phase on the calculation of pseudo-static earth pressure on a retaining wall. Geotechnique 40, 1, 103-112. DOI: 10.1680/geot.1990.40.1.103
[9] Richards, R., Elms, D. 1979. Seismic Behavior of Gravity Retaining Walls. J. Geotech Eng. 105(GT4), 449-464.
[10] Richards, R., Elms, D. 1990. Seismic Design of Retaining Walls. Proc. of ASCE Specialty Conf. on Design and Performance of Earth Retaining Structures, Geotechnical Special Publication 25, 854-871.
[11] Richards, R., Shi, X. 1994. Seismic lateral pressures in soils with cohesion. J. Geotech. Eng. 120, 7, 1230–1251. DOI: 10.1061/(ASCE)0733-9410(1994)120:7(1230)
[12] Velesos, A.S., Younan, A.H. 1994. Dynamic Modeling and Response of Soil-Wall Systems. J. Geotech. Eng. 120, 12, 2155-2179. DOI: 10.1061/(ASCE)0733-9410(1994)120:12(2155)
[13] Morrison, E.E., Ebeling, R.M. 1995. Limit equilibrium computation of dynamic passive earth pressure. Can. Geotech. J. 32, 481-487. DOI: 10.1139/t95-050
[14] Soubra, A.H. 2000. Static and seismic passive earth pressure coefficient on rigid retaining structures. Can. Geotech. J. 37, 463-478. DOI: 10.1139/t99-117
[15] Chen, Y. 2000. Practical analysis and design of mechanically-stabilized earth walls-I. Design philosophies and procedures Eng. Struct. 22, 7, 793-808. DOI: 10.1016/S0141-0296(99)00021-8
[16] Kumar, J. 2001. Seismic passive earth pressure coefficient for sands. Can. Geotech. J. 38, 876-881. DOI: 10.1139/t01-004
[17] Kumar, J., Chitikela, S. 2002. Seismic passive earth pressure coefficient using the method of characteristics. Can. Geotech. J. 39, 463-471. DOI: 10.1139/t01-103
[18] Green, R.A., Ebeling, R.M. 2002. Seismic analysis of cantilever retaining walls, Phase I. ERDC/ITL TR-02-3. Information technology laboratory, US army corps of engineers, Engineer research and development center, Vicksburg, MS.
[19] Saran, S., Gupta, R.P. 2003. Seismic Earth Pressure behind Retaining Walls. Indian. Geotech. J. 33, 3, 195-213.
[20] Cheng, Y.M. 2003. Seismic lateral earth pressure coefficients for C-φ soils by slip line method. J. Comput. Geotech. 30, 7, 661-670. DOI: 10.1016/j.compgeo.2003.07.003
[21] Yang, X.L, Yin, J.H. 2006. Estimation of seismic passive earth pressure with nonlinear failure criterion. Eng. Struct. 28, 342-348. DOI: 10.1016/j.engstruct.2005.08.007
[22] Choudhury, D., Nimbalkar, S.S. 2006. Psuedo-dynamic approach of seismic active earth pressure behind retaining wall. J. Geotech. Geolog. Eng. 24, 5, 1103-1113. DOI: 10.1007/s10706-005-1134-x
[23] Mylonakis, G., Kloukinas, P, Papatonopoulos, C. 2007. An alternative to the Mononobe-Okabe equation for seismic earth pressures. Soil. Dyn. Earthq. Eng. 27, 10, 957-969. DOI: 10.1016/j.soildyn. 2007.01.004
[24] Ghanbari, A, Ahmadabadi, M. 2010. Active earth pressure on inclined retaining walls in static and Psuedo-static condition. Int. J. Civil Eng. 8, 2, 159-172.
[25] Lambe, T.W., Whitman, R.V. 1979. Soil mechanics. SI version, Wiley, New York.
[26] Das, B.M. 1998. Principles of geotechnical engineering. Fourth Ed. PWS, Boston.